$$\tau = \begin{cases} k & 0 < l < l_c \\ \\ \mu\sigma & l_t < l \leq l_c \end{cases} \tag{7}$$

Also, from Fig. 1, the following can be written

$$F_c = R\cos(\lambda - \alpha) \tag{8}$$

$$F_t = R\sin(\lambda - \alpha) \tag{9}$$

$$F_s = K_{AB} lw \tag{10}$$

$$N = R\cos\lambda \tag{11}$$

$$F = R\sin\lambda \tag{12}$$

where

$$R = \frac{F_s}{\cos\theta} = \frac{K_{AB} tw}{\sin\phi\cos\theta} \tag{13}$$

Following Eqns. (9) - (13), an expression for the friction coefficient is

$$\mu = \frac{F_t}{F_r} = \frac{R\sin(\lambda - \alpha) + R\cos(\lambda - \alpha)\tan\alpha}{R\cos(\lambda - \alpha) - R\sin(\lambda - \alpha)\tan\alpha} \tag{14}$$

which gives

$$\mu = \frac{\sin(\lambda - \alpha) + \cos(\lambda - \alpha)\tan\alpha}{\cos(\lambda - \alpha) - \sin(\lambda - \alpha)\tan\alpha} \tag{15}$$

In this work, an improved model of Johnson-Cook flow stress is developed, the shear force can be written as

$$\sigma_{AB} = \sigma_m + \left(\sigma_0 + B\varepsilon_{AB}^n\right)\left(1 + C\log\frac{\dot{\varepsilon}_{AB}}{\dot{\varepsilon}_0}\right)\left(1 - \left(\frac{T - T_r}{T_m - T_r}\right)^m\right) \tag{16}$$

Recall that the frictional force is given as

$$F_{AB} = F_s = \mu\sigma_{AB} \tag{17}$$

Therefore, from Eqns. (15), (16) and (17), the frictional force is

$$F_{AB} = \left[\frac{\sin(\lambda - \alpha) + \cos(\lambda - \alpha)\tan\alpha}{\cos(\lambda - \alpha) - \sin(\lambda - \alpha)\tan\alpha}\right]\left\{\sigma_m + \left(\sigma_0 + B\varepsilon_{AB}^n\right)\left(1 + C\log\frac{\dot{\varepsilon}_{AB}}{\dot{\varepsilon}_0}\right)\left(1 - \left(\frac{T - T_r}{T_m - T_r}\right)^m\right)\right\} \tag{18}$$

Where, *T* determined from the temperature rise along the shear zone (X, Z) can be calculated as;

$$T_{chip-shear}(X, Z) = \frac{q_{shear}}{2\pi k_{chip}} \left[\int_0^{l_i} e^{-\frac{(x - x_i)V_{chip}}{2a_{chip}}} \left[\begin{array}{l} k_0\left(\frac{V_{chip}}{2a_{chip}}\sqrt{(X - X_i)^2 + (Z - Z_i)^2}\right) + \\ \frac{1}{2}k_0\left(\frac{V_{chip}}{2a_{chip}}\sqrt{(X - X_i)^2 + (2t_{chip} - Z - Z_i)^2}\right) + \\ \frac{1}{2}k_0\left(\frac{V_{chip}}{2a_{chip}}\sqrt{(X - X_i)^2 + (Z - Z_i)^2}\right) \end{array}\right] dl_i\right] \tag{19}$$

where

$$X_i = l - l_i\sin(\phi - \alpha) \qquad Z_i = l_i\cos(\phi - \alpha) \qquad l = \frac{t_{chip}}{\cos(\phi - \alpha)}$$

For the frictional force at tool-chip interface, the temperature rise along the tool-chip interface is

$$T_{tool-chip}(X, Y, Z') = \frac{1}{2\pi k_{tool}}\int_0^h \left[1 - B(x)\right] q_{friction}\, dx \int_{-b}^{b}\left(\frac{1}{R_i} + \frac{1}{R_i'}\right) dy \tag{20}$$

where

$$R_i = \sqrt{\left(X - x_i\right)^2 + \left(Y - y_i\right)^2 + Z'^2} \qquad R_i' = \sqrt{\left(X - 2h + x_i\right)^2 + \left(Y - y_i\right)^2 + Z'^2}$$

$$q_{shear} = \frac{F_s V_s}{lw} \qquad q_{friction} = \frac{F V_{chip}}{hw}$$

Based on the temperature rise profiles along the primary shear zone and tool-chip interface, the average temperatures are categorized as

$$T_{shear-average} = T_0 + \frac{\int_0^l T_{chip-shear}\left(X, Z\right) dl_i}{l} \tag{21}$$

and

$$T_{tool-chip} = T_0 + + \frac{\int_0^{h_n} T_{chip-shear}\left(X, 0, 0\right) dX}{h} \tag{22}$$

The calculated average temperature is used to compute the flow stress along the primary shear zone and at the tool-chip interface.
It should be noted that the normal stress acting on the tool-chip interface is

$$\sigma_N = \tau_{AB}\left(1 + 2\left(\frac{\pi}{4} - \alpha\right) - \frac{2c\gamma_{At} I}{K_{AB}}\right) \tag{23}$$

where

$$I = \left(\frac{\partial \tau}{\partial \gamma}\right)_{AB} = \frac{\partial \tau}{\partial \varepsilon}\frac{\partial \varepsilon}{\partial \gamma} + \frac{\partial \tau}{\partial T}\frac{\partial T}{\partial \gamma} \tag{24}$$

where

$$\tau = \left[\frac{\sin\left(\lambda - \alpha\right) + \cos\left(\lambda - \alpha\right)\tan\alpha}{\cos\left(\lambda - \alpha\right) - \sin\left(\lambda - \alpha\right)\tan\alpha}\right]\left\{\sigma_m + \left(\sigma_0 + B\varepsilon_{AB}^n\right)\left(1 + C\log\frac{\dot{\varepsilon}_{AB}}{\dot{\varepsilon}_0}\right)\left(1 - \left(\frac{T - T_r}{T_m - T_r}\right)^m\right)\right\} \tag{25}$$

From Eqns. (24) and (25), *I* become

$$I = \left[\frac{\sin\left(\lambda - \alpha\right) + \cos\left(\lambda - \alpha\right)\tan\alpha}{\cos\left(\lambda - \alpha\right) - \sin\left(\lambda - \alpha\right)\tan\alpha}\right]\left\{\begin{array}{l}\left(nB\varepsilon_{AB}^{n-1}\right)\left(1 + C\log\frac{\dot{\varepsilon}_{AB}}{\dot{\varepsilon}_0}\right)\left(1 - \left(\frac{T - T_r}{T_m - T_r}\right)^m\right) \\ -m\left\{\sigma_m + \left(\sigma_0 + B\varepsilon_{AB}^n\right)\left(1 + C\log\frac{\dot{\varepsilon}_{AB}}{\dot{\varepsilon}_0}\right)\left(\frac{T - T_r}{T_m - T_r}\right)^{m-1}\right\}\frac{dT}{d\gamma}\end{array}\right\} \tag{26}$$

Maximum shear and shear strain rate at the tool-chip interface are given respectively as

$$\gamma = \frac{1}{2}\left(\frac{\cos\alpha}{\sin\phi\cos\left(\phi - \alpha\right)}\right) \tag{27}$$

$$\dot{\gamma}_{\text{int}} = \frac{V_{chip}}{\delta t_{in}} \tag{28}$$

It should be noted that

$$\dot{\gamma}_{AB} = C\frac{V_s}{l} \tag{29}$$

where

$$V_s = \frac{V_c \cos\alpha}{\sin\phi\cos\left(\phi - \alpha\right)} \tag{30}$$

Therefore,

$$\dot{\gamma}_{AB} = \frac{C}{l}\frac{V_c \cos\alpha}{\cos(\phi-\alpha)} \tag{31}$$

Where, ϕ can be numerically determined using Oxley's model (1961)

$$\phi = a\tan\left[1+\frac{\pi}{2}-2\phi+\frac{\cos 2(\phi-\gamma)}{\tan\rho}-\sin 2(\phi-\gamma)\right]-(\rho-\gamma) \tag{32}$$

And the friction angle as

$$\tan\theta = 1+2\left(\frac{\pi}{4}-\phi\right)-\frac{c\gamma_{At}I}{K_{AB}} \tag{33}$$

3. Results and Discussion

Figures 2a-c show the comparison of the experimental results of Xu et al. (2010) with the present developed models. The model results cutting and tangential forces are compared with the experimental results as shown in Fig. 2. Fig. 2b presents the comparison of the experimental results of cutting stress with the results of the cutting stress in the present developed models while Fig. 1c displays the comparison of the experimental results of cutting temperature with the results of the cutting temperature in the present developed models. Also, the effects of coefficient of friction on the forces, cutting stress and temperature are presented. It is depicted that the coefficient of friction has direct relationship on the forces, cutting stress and temperature in a way that as coefficient of friction increases, the forces, cutting stress and temperature increase. This is because as the coefficient of friction increase, the frictional force that enhances the cutting process increases which consequently increase the cutting stress and more heat are generated in the material and the cutting zone thereby the cutting temperature is increased.

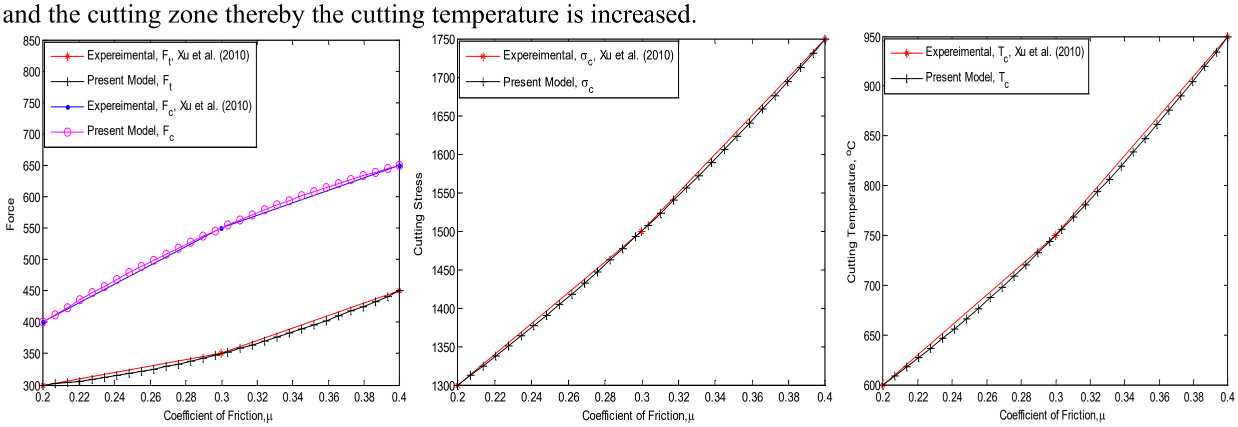

Figure 2. Model results of (a) cutting and tangential forces; (b) cutting stress; (c) cutting temperature

Figure 3 shows the effect of temperature on the flow stress. It is shown that as the temperature increases, the flow stress decreases. It is shown that increase in temperature results in decrease in flow stress due to softening effects on the material. Also, it is established that the cutting action and related friction at cutting surfaces increase the temperature of the tool material, which further accelerates the physical and chemical processes associated with tool wear. In order to remove the unwanted material as chips, these forces and motions are necessary; therefore, cutting tool wear is an economic penalty that must be accounted for in order to machine the part. The magnitude of this economic penalty can be minimized if the cutting process is planned and controlled based on sound knowledge of the cutting engagement, wear process and its dependency on the selection of cutting conditions. The cutting conditions normally controlled are the engagement of the cutting edge with the workpiece, the relative velocity of the cutting edge with the workpiece, and the feed velocity used to keep the tool engaged into uncut material. During the process planning stage, an assessment must be made concerning how difficult the material is to machine, the correct tool for the surface to be created must be selected, the appropriate tool material must be selected, and the type of cutting fluid needed must be determined. To make such choices, the wear environment in metal cutting must be understood and the related friction must be analyzed as carried in the present study.

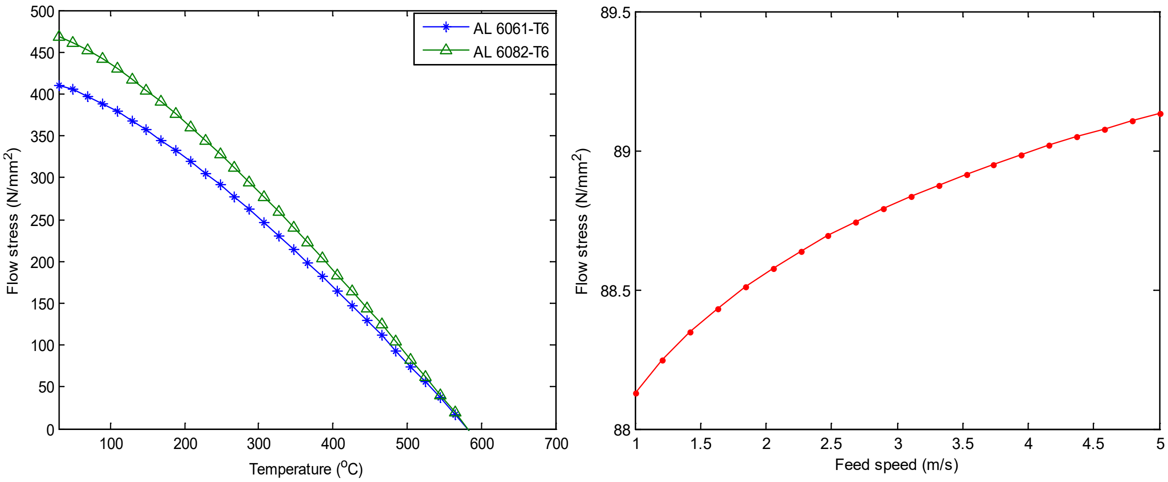

Figure 3. Effects of Temperature on the flow stress

Fig. 4 illustrates the variation of the tool rake angle with the flow stress. It shows that as the rake angle moves from the negative angle to zero, the flow stress reduces. It is clearly seen that the increase of cutting speed, feed rate and axial depth causes the friction stress increase dramatically. Meanwhile, the friction coefficient, angle and force increases with decreases of feed rate and increases of cutting speed and axial depth. It is established in literature that that the feed rate was the most dominant cutting condition on the cutting force, followed by the axial depth, radial depth of cut and then by the cutting speed. The cutting force increases with increasing the feed rate, depths of cut but decreases with increasing cutting speed.

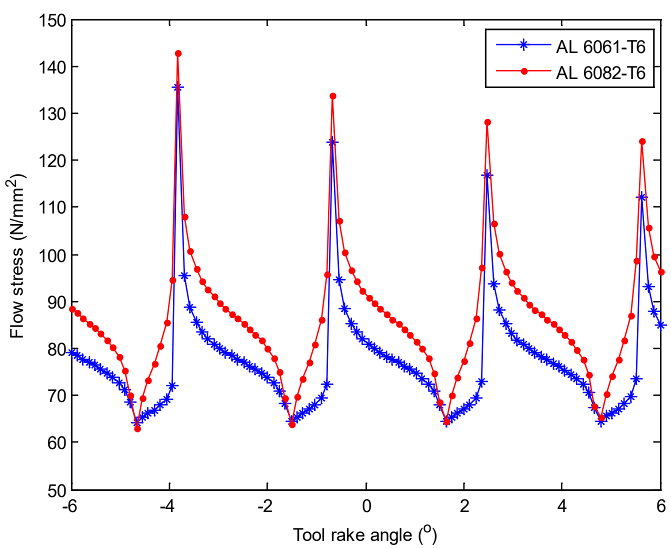

Figure 4. Effects of tool rake angle on the flow stress for the two types on aluminum

4. Conclusion

In this work, effects of friction on the machining process during orthogonal cutting has been theoretically investigated. Mathematical models were developed and parametric studies of the effects of friction and cutting force parameters on the machining process were carried out. The developed models were validated. It was established that as coefficient of friction increases, the forces, cutting stress and temperature increase. The frictional shear stress directly proportional to the normal stress increases. However, the frictional stress increases as the coefficient of friction increases. Also, the present work revealed that as the temperature increases, the flow stress decreases. Furthermore, it is shown that as the feed speed increases, there is an increase in the flow stress of the material used. The cutting force increases with increasing the feed rate, depths of cut but decreases with increasing cutting speed. This work will enhance the understanding of the influences of friction coefficient on the cutting process and also assist in the development of good products with good surface finish.

References

Abukhshim, N.A, Mativenga, P.T and Sheikh, M.A., Heat generation and temperature prediction in metal cutting: A review and implications for high speed machining, *International Journal of Machine Tools & Manufacture*, vol. 46, pp. 782–800, 2006.

Abdelali, B., Claudin, C., Rech, J., Experimental characterization of friction coefficient at the tool-chip-workpiece interface during dry machining of AISI 1045, *Wear*, vol. *286-287*, pp. 108-115, 2012.

McClain, B., Stephen, A., Batzer, G. Ivan Maldonado, A numeric investigation of the rake face stress distribution in orthogonal machining, *Journal of Material Processing Technology,* vol. 123, pp. 114-119, 2002.

Brocail, J., Laurent, D., Watremez, M., Identification of a friction model for modeling of orthogonal cutting, *International Journal. Mach. Tool Manuf*, vol. 50, pp. 807–814, 2010.

El Hakim, M.A. Shalaby, M.A, Veldhuis, S.C., Dosbaeva, G.K., Effect of secondary hardening on cutting forces, cutting temperature, and tool wear in hard turning of high alloy tool steels, *Measurement*, vol. 65, pp. 233–238, 2015.

Fang, N., Machining with tool–chip contact on the tool secondary rake face - Part I: A slip-line model, *International Journal of Mechanical Sciences,* vol. 44 pp. 2337–2354, 2002.

Fang, N., Jawahir, I.S., A new methodology for determining the stress state of the plastic region in machining with restricted contact tools, *International Journal Mechanical Science*, vol. 43, pp. 1747-1770, 2001.

Guoqin, S., Xiaomin, D., Chandrakanth, S. A., Finite element study of the effect of friction in orthogonal metal cutting, *Finite Elements in Analysis and Design*, vol. 38, no. 9, pp. 863–883, 2002.

Jaspers, P. F. C and Dautzenberg, J.H., Material behaviour in metal cutting: strain rates and temperatures in chip formation, *Journal of Materials Processing Technology*, vol. 121, no. 1, pp. 123-135, 2002.

Karpat, Y., Ozel, T., Predictive Analytical and thermal Modeling of Orthogonal Cutting Process Part 1: Predictions of Tool Forces, stresses, and Temperature Distributions, *J. Manuf. Sci. Eng.*, vol. 128, pp. 435-444, 2006.

Lin, Z.C., Pan, W.C., Lo., A study of orthogonal cutting with tool flank wear and sticking behavior on the chip-tool interface, *J. Mat. Proc. Tech*., vol. 52, pp. 524-538, 1995.

Maity, K.P., Das, N.S., A Class of slip line field solutions for metal machining with sticking-slipping zone including elastic contact, *Mater. Design,* doi:10.1016/j.matdes, 2006.

Merchant, M. E., Mechanics of the metal cutting process I: Orthogonal cutting and a type 2 chip, *Journal of Applied Physics*, vol. 16, no. 5, pp. 267-275, 1945.

Moufki, A., Alain Molinari, Dudzinski, D., Modelling of Orthogonal Cutting with a Temperature Dependent Friction Law, *Journal of the Mechanics and Physics of Solids*, vol. 46, no. 10, pp. 2103-2138, 1998.

Mustafa, G., Ihsan, K., Ersan, A., Ulvi, S., Experimental investigation of the effect of cutting tool rake angle on main cutting force, *Journal of Materials Processing Technology*, vol. 166, pp. 44-49, 2005.

Oxley, P., Mechanics of metal cutting, *International Journal of Machine Tool Design and Research,* vol. 1, nos. 1-2, 89-97, 1961.

Ozel, T., The influence of friction models on finite element simulations of machining, *J. Machine Tools & Manufacture*, vol. 46, pp. 518-530, 2006.

Zhenhua, T., Yang, J.C., Lovell, M.R., Evaluation of interfacial friction in material removal processes: the role of workpiece properties and contact geometry, *Wear*, vol. 256, no. 7, 664-670, 2004.

Xu, G. T. and Li, Y. S., Numerical Modeling the Effect of Tool-Chip Friction in Orthogonal Cutting AISI4340, *Applied Mechanics and Materials,* vols. 29-32, 1815-1819, 2010.

Biographies

Sunday Joshua Ojolo is an Associate Professor of Machine Design and Manufacturing Engineering in University of Lagos since 2016.His area of specialisation is in machinery development, manufacturing engineering and energy systems. He has published over 70 research papers in reputable journals. He is a member of America Society of Mechanical Engineers, Nigerian Society of Engineers; a Fellow at Nigerian Institution of Mechanical Engineering; COREN Registered Engineer. He is on the editorial board of five reputable international journals. He is a consultant to many industries.

Gbeminiyi Musbau Sobamowo is a Senior Lecturer in Themo-fluids at the University of Lagos. His area of specialisation is in thermal sciences, energy studies and modelling. He is a member of the Nigeria Society of Engineers and registered Engineer with COREN. He has published over 40 reasearch articles majorly in international journals.

Mercy Adedayo is a Principal Engineer in the Department of Works and Services at the University of Lagos. She holds a masters degree in Mechanical Engineering. Her area of specialisation is Manufacturing Engineering.